

## Oxidative Stress-Induced Metabolic Changes in Mouse C2C12 Myotubes Studied with High-Resolution $^{13}\text{C}$ , $^1\text{H}$ , and $^{31}\text{P}$ NMR Spectroscopy

IDA K. STRAADT,<sup>†</sup> JETTE F. YOUNG,<sup>†</sup> BENT O. PETERSEN,<sup>‡</sup> JENS Ø. DUUS,<sup>‡</sup>  
NIELS GREGERSEN,<sup>§</sup> PETER BROSS,<sup>§</sup> NIELS OKSBJERG,<sup>†</sup> PETER K. THEIL,<sup>||</sup> AND  
HANNE C. BERTRAM<sup>\*,\dagger</sup>

<sup>†</sup>Department of Food Science, Faculty of Agricultural Sciences, Aarhus University, Blichers Allé 20, P.O. Box 50, DK-8830 Tjele, Denmark, <sup>‡</sup>Carlsberg Laboratory, Gamle Carlsberg Vej 10, DK-2500 Valby, Denmark, <sup>§</sup>Research Unit for Molecular Medicine, Aarhus University, Brendstrupgaardsvej 100, DK-8200, Aarhus N, Denmark, <sup>||</sup>Department of Animal Health, Welfare and Nutrition, Faculty of Agricultural Sciences, Aarhus University, Blichers Allé 20, P.O. Box 50, DK-8830 Tjele, Denmark, and <sup>\dagger</sup>Department of Food Science, Faculty of Agricultural Sciences, Aarhus University, Kirstinebjergvej 10, DK-5792 Aarslev, Denmark

In this study, stress in relation to slaughter was investigated in a model system by the use of  $^{13}\text{C}$ ,  $^1\text{H}$ , and  $^{31}\text{P}$  nuclear magnetic resonance (NMR) spectroscopy for elucidating changes in the metabolites in C2C12 myotubes exposed to  $\text{H}_2\text{O}_2$ -induced stress. Oxidative stress resulted in lower levels of several metabolites, mainly amino acids; however, higher levels of alanine were apparent in the  $^{13}\text{C}$  spectra after incubation with [ $^{13}\text{C}_1$ ]glucose. In the  $^{13}\text{C}$  spectra [ $^{13}\text{C}_3$ ]lactate tended to increase after exposure to increasing concentrations of  $\text{H}_2\text{O}_2$ ; conversely, a tendency to lower levels of the unlabeled ( $^{12}\text{C}$ ) lactate were identified in the  $^1\text{H}$  spectra after stress exposure. These data indicate an increase in de novo synthesis of alanine, concomitant with a release of lactate from the myotubes to the medium at oxidative stress conditions. The changes in the metabolite levels could possibly be useful as markers for meat quality traits.

**KEYWORDS:** Metabolomics; nuclear magnetic resonance; HO-1; Hox1; heat shock protein; alanine; creatine phosphate; lactate; hydrogen peroxide; muscle cells

### INTRODUCTION

When handling pigs in relation to slaughter, ante and post mortem stress factors influence the subsequent meat quality. Preslaughter conditions can lead to an increase in the body temperature, thereby resulting in heat stress (1–3). Likewise, stunning and exsanguination in connection with the actual slaughter process cause anoxia and disruption of the energy supply to the muscle cells (4, 5). Physical stress exposure also affects the glycogen content as well as the rate of glycolysis and hence the pH development post mortem, and it has been found that pH, temperature, and the metabolites lactate and ATP measured early post mortem are good indicators for the subsequent meat quality development (6, 7). However, the fundamental cellular mechanisms in relation to these stressors have not been well described but could be further investigated in muscle cell cultures, where stressors can be studied separately under controlled conditions. Differentiated muscle cell cultures have been used for studying responses to anoxia and  $\text{H}_2\text{O}_2$ -induced oxidative stress in the mouse muscle cell line C2C12 (8–11) and in primary porcine muscle cells (12). Applying a muscle model system is associated with certain limitations in comparison to

whole animal studies. Draining of the blood from the muscle after slaughter causes ischemic anoxia, and anaerobic end products such as lactate cannot leave the muscle, while external fuels (i.e., glucose) cannot be delivered in the absence of blood flow post mortem. These exact conditions cannot be simulated in a muscle model (13). However, a previous study with the muscle model system C2C12 has shown that exposure of the myotubes to anoxia and a pH decrease to simulate the events taking place at the time of slaughter influence cellular events of importance for drip loss (11). Hence, differentiated muscle cell cultures may provide a valuable tool for studying basic cellular mechanisms involved in other ante and post mortem processes. Both heat stress and anoxia, occurring in relation to slaughter, can result in oxidative stress (14). Hence, in the present study we have used myotubes derived from the mouse muscle cell line C2C12 as a model system for skeletal muscle cells in order to investigate the effects of oxidative stress at the cellular level. Nuclear magnetic resonance (NMR)-based spectroscopy has proven useful in several studies on tissue samples from animals: e.g., different combinations of preslaughter stress and stunning methods have been distinguished by  $^{13}\text{C}$  magic angle spinning (MAS) NMR and  $^{31}\text{P}$  NMR spectroscopy in post mortem muscle tissue samples (15–17). In pigs exposed to treadmill stress a possible relation between degradation of creatine and formation of lactate

\*To whom correspondence should be addressed. Tel: +45 8999 3344. Fax: +45 8999 3495. E-mail: HanneC.Bertram@agrsci.dk.

was found by application of solid-state MAS  $^{13}\text{C}$  NMR spectroscopy in post mortem muscles (17), whereas lower levels of the high-energy phosphate ATP in the muscles post mortem have been observed by use of  $^{31}\text{P}$  NMR spectroscopy after exposure to high-stress stunning methods, in comparison to control pigs (15, 18). In contrast, few but promising studies with NMR applications on cell cultures have been performed (19–22), and to the authors' knowledge NMR studies on cells in relation to slaughter stress have not been carried out before. We hypothesize that NMR-based metabonomics is an eminent and informative tool for detailed studies on stress response in cell cultures. Thus, the overall aim of the present study was to explore the use of  $^{13}\text{C}$ ,  $^1\text{H}$ , and  $^{31}\text{P}$  NMR spectroscopy for elucidating changes in the metabolites in C2C12 myotubes exposed to  $\text{H}_2\text{O}_2$ -induced stress. The optimal oxidative stress conditions in the myotube model were evaluated by a viability test and by determination of the mRNA level and the expression level of the heat shock protein heme oxygenase-1 (HO-1).

## MATERIALS AND METHODS

**Muscle Cell Cultures.** The mouse myoblast cell line C2C12, originally derived from a mouse thigh muscle (23) (American Type Culture Collection, Manassas, VA), was grown to establish myotube cultures. Briefly, a clone that effectively fuses and forms myotubes was grown in a 75  $\text{cm}^2$  culture flask in 10 mL of growth medium consisting of Dulbecco's Modified Eagle's Medium (DMEM; Invitrogen, Paisley, U.K.), 10% (v/v) fetal calf serum (FCS), 100 IU/mL penicillin, 100  $\mu\text{g}/\text{mL}$  streptomycin, 3  $\mu\text{g}/\text{mL}$  amphotericin B, and 20  $\mu\text{g}/\text{mL}$  gentamycin. Cells were maintained in an atmosphere of 95% air and 5%  $\text{CO}_2$  at 37  $^\circ\text{C}$ . Prior to confluence, cells were harvested in 0.25% trypsin and seeded in 96-well plates, 24-well plates, or Petri dishes (140 mm in diameter) at a density of 10 000 cells/ $\text{cm}^2$ . Cells were grown to confluence in growth medium and left to fuse in differentiation medium containing DMEM, 4% (v/v) FCS, and amounts of antibiotics similar to those in the growth medium. After ~4 days, the cultures contained differentiated multinuclear myotubes and were ready for experimental use.

**Experimental Setup and Analysis of Myotube Viability.** Viability of the C2C12 myotubes was evaluated in 96-well plates by WST-1 (Roche, Hvidovre, Denmark), which is a formazan salt that is cleaved by mitochondrial dehydrogenase of viable cells. The myotubes were incubated for 1 h in Krebs-HEPES buffer with  $\text{H}_2\text{O}_2$  concentrations between 0 and 300  $\mu\text{M}$ . The  $\text{H}_2\text{O}_2$  concentration was adjusted by measuring the absorbance at 240 nm. The myotubes were washed with phosphate-buffered saline (PBS) and incubated in differentiation medium with 10  $\mu\text{L}/\text{well}$  WST-1 for 4 h. The relative amount of viable cells was determined by measuring the absorbance at 450 nm. Data were corrected by subtracting the background absorbance of the medium alone. All concentrations of  $\text{H}_2\text{O}_2$  were determined in quadruplicate wells ( $n = 4$ ).

**Experimental Setup, RNA Extraction, Real Time RT-PCR, Protein Extraction, and Western Blot.** For real time reverse transcription polymerase chain reaction (RT-PCR) and Western blot analysis the myotubes were incubated in 24-well plates with Krebs-HEPES buffer without  $\text{H}_2\text{O}_2$  or with 100  $\mu\text{M}$   $\text{H}_2\text{O}_2$  for 1 h. After incubation the myotubes were washed with PBS and incubated with fresh differentiation medium. Myotubes were harvested in 0.25% trypsin immediately after the incubation in Krebs-HEPES buffer without  $\text{H}_2\text{O}_2$  (control) and at different time points after the incubation in Krebs-HEPES buffer with 100  $\mu\text{M}$   $\text{H}_2\text{O}_2$ . The harvested myotubes were stored in Eppendorf tubes at  $-80^\circ\text{C}$  until extraction of RNA or protein.

The RNA was purified using the AllPrep RNA/protein kit (Qiagen, Albertslund, Denmark), and the RNA concentration was determined after dilution by measuring the absorbance at 260 nm (A260). After the RNA concentrations of all the samples were adjusted to the same level (9  $\text{ng}/\mu\text{L}$ ), which is one of the normalization procedures recommended by Bustin (24), the RNA was reverse-transcribed with oligo-dT primers and a Superscript II RNase H reverse transcriptase kit (Invitrogen, Taastrup, Denmark). Reverse-transcribed material (1  $\mu\text{L}$ ) was amplified with TaqMan Universal PCR Master Mix (Applied Biosystems, Stockholm, Sweden). The quantity of HO-1 mRNA was detected with the commercial TaqMan gene

expression assay (Applied Biosystems, Stockholm, Sweden) with two unlabeled PCR primers and one FAM dye-labeled TaqMan MGB probe specific for the mouse (*Mus musculus*) HO-1 gene (Mm00516005\_m1). For PCR, 40 cycles at 95  $^\circ\text{C}$  for 15 s and 60  $^\circ\text{C}$  for 60 s were applied to amplify the PCR products. A selected sample was diluted serially and analyzed in triplicate to test the linearity and efficiency of the PCR amplifications. Furthermore, control wells with either water or genomic mouse DNA were used as negative controls. The samples were analyzed using an ABI 7900HT detection system (Applied Biosystems, Stockholm, Sweden). To evaluate mRNA quantities, data were obtained as  $C_t$  values (the cycle number at which logarithmic plots cross a calculated threshold line). The relative mRNA quantity was calculated using the following formula: relative quantity =  $2^{-\Delta C_t}$ , where the mRNA level is expressed relative to cells without stress. At each time point myotubes were harvested from 2 wells ( $n = 2$ ) and analyzed for HO-1 mRNA in duplicate.

For protein extraction the harvested myotubes were washed three times with PBS and dissolved in buffer (0.125 M Tris, 4% SDS, 20% glycerol, 0.1 M DTE). Samples harvested from two wells were pooled, homogenized with a sonicator (20 cycles, amplitude 80%, cycle 0.75 s) and centrifuged at 14 000g for 30 min. The supernatant was transferred to a new tube, and the protein concentration was determined by measuring the absorbance at 280 nm (A280). Samples were heated for 10 min in a 60  $^\circ\text{C}$  heating block before loading a volume equal to 150  $\mu\text{g}$  of protein in each lane. The samples were loaded on a 10%, 18-well Criterion gel (BioRad Laboratories, CA) and run at 200 V for 1 h at room temperature, and the proteins were transferred from the gel to a polyvinylidene fluoride membrane (25). The proteins were transferred at 150 V and 1.5 mA for 1.5 h at 5  $^\circ\text{C}$  with gentle stirring. The membrane was rinsed with deionized water and blocked in Tween-Tris-buffered saline (TTBS) with 5% nonfat dry milk (BioRad Laboratories, CA) overnight at 4  $^\circ\text{C}$ . The membrane was washed twice for 10 min in TTBS and incubated for 2 h at room temperature with the anti-HO-1 primary antibody (rabbit anti-HO-1, Calbiochem, Darmstadt, Germany) diluted 1:2000 in TTBS. The membrane was washed six times for 5 min in TTBS and incubated 1 h at room temperature with the Alexa Flour 488 goat-antirabbit labeled secondary antibody (Invitrogen, Taastrup, Denmark) diluted 1:2000 in TTBS. Subsequently the membrane was washed twice for 10 min and four times for 5 min in TTBS before a final rinse with water. The membrane was scanned with an image scanner (Molecular Imager FX, Bio-Rad).

**$^{13}\text{C}$  Enrichment and Extraction of Cells for NMR Spectroscopic Analysis.** To a differentiation medium made from glucose-free DMEM (Invitrogen, Cat. No. 11966-025) and to Krebs-HEPES buffer was added 5.5 mM [ $^{13}\text{C}_1$ ]glucose (Cambridge Isotope Laboratories, Andover, MA). The myotube cultures grown in Petri dishes were incubated for 4 h with 5.5 mM [ $^{13}\text{C}_1$ ]glucose (a) for 1 h in Krebs-HEPES buffer followed by 3 h in the medium, (b) for 1 h with Krebs-HEPES buffer containing 100  $\mu\text{M}$   $\text{H}_2\text{O}_2$ , followed by 3 h in the medium, or (c) with Krebs-HEPES buffer containing 500  $\mu\text{M}$   $\text{H}_2\text{O}_2$  for 1 h, followed by 3 h in the medium. After the 4 h incubation with 5.5 mM [ $^{13}\text{C}_1$ ]glucose, the [ $^{13}\text{C}_1$ ]glucose-containing medium was discarded, the cells were washed three times with an ice-cold 0.9% NaCl solution to remove excess medium, and the cells were subsequently frozen in liquid nitrogen. For extraction of the cells a methanol/chloroform extraction method previously described (22) was applied. After the extraction the samples were freeze-dried at  $-80^\circ\text{C}$  and stored at  $-80^\circ\text{C}$  until NMR analysis.

**NMR Spectroscopy.** The freeze-dried methanol/water phase from the cell extracts were dissolved in 600  $\mu\text{L}$  of  $\text{D}_2\text{O}$  containing 0.025% (w/v) sodium trimethylsilyl[2,2,3,3- $\text{D}_4$ ]-1-propionate (TSP) and 0.01% (v/v) dioxane.  $^{13}\text{C}$  and  $^1\text{H}$  NMR spectra of the cell extracts were recorded at 25  $^\circ\text{C}$  on a Bruker Avance 800 spectrometer, operating at a  $^{13}\text{C}$  frequency of 201.01 MHz and a  $^1\text{H}$  frequency of 799.40 MHz, equipped with a 5 mm  $^1\text{H}$  observe cryoprobe (Bruker BioSpin, Rheinstetten, Germany). Proton-decoupled  $^{13}\text{C}$  NMR spectra were recorded using Bruker standard homonuclear pulse programs, and each spectrum was the sum of 1024 free induction decays (FID). A 90 $^\circ$  pulse was applied with a repetition time of 3 s and an acquisition time of 0.682 s. Standard one-dimensional (1D)  $^1\text{H}$  NMR spectra were acquired using a single 90 $^\circ$  pulse experiment, and each spectrum was the sum of 16 FIDs. Water suppression was achieved by irradiating the water peak during the relaxation delay of 5 s, and 32 K data points spanning a spectral width of 13.03 ppm were collected. In addition,  $^{13}\text{C}$ -decoupled  $^1\text{H}$  NMR spectra were recorded to verify the assignment of

signals from  $^{13}\text{C}$ -labeled metabolites in the  $^1\text{H}$  NMR spectra. All spectra were referenced to TSP at 0 ppm. Dioxane ( $\delta$  69.44 ppm) was used as a secondary reference in the  $^{13}\text{C}$  NMR spectra. In addition, to aid assignment, two-dimensional (2D)  $^1\text{H}$ - $^1\text{H}$  COSY and 2D  $^1\text{H}$ - $^{13}\text{C}$  HSQC spectra were recorded on selected cell samples using water suppression.  $^{13}\text{C}$  and  $^1\text{H}$  NMR spectra were obtained on three replicates ( $n = 3$ ), each

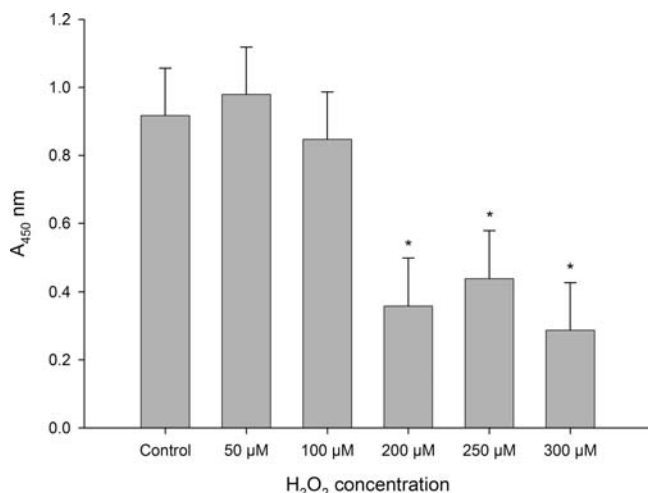


**Figure 1.** Viability of C2C12 myotubes after exposure to different concentrations of  $\text{H}_2\text{O}_2$  for 1 h. LSMeans ( $n = 4$ ) and SEM of  $A_{450}$  nm of the WST-1 assay are given. Values significantly different from the control are indicated by an asterisk ( $P < 0.05$ ).

represented by the freeze-dried methanol/water phase from the cell extract from one Petri dish, of each treatment group (a–c) described above.

$^{31}\text{P}$  NMR spectra were recorded at 25 °C on a Bruker Avance III 600 spectrometer (Bruker BioSpin, Rheinstetten, Germany), operating at a  $^{31}\text{P}$  frequency of 242.94 MHz. The  $^{31}\text{P}$  NMR spectra were obtained as the sum of 8192 FIDs acquired with a repetition time of 5 s and an acquisition time of 1.346 s. The width was 12 kHz, and the chemical shift was referenced to PCr at 0 ppm.  $^{31}\text{P}$  NMR spectra were obtained on samples of the treatment groups a and c described above.

Quantification of the various metabolites was carried out by integration of peak areas using Topspin 2.1 software (Bruker BioSpin, Rheinstetten, Germany). The  $^{13}\text{C}$  NMR spectra were integrated in the range 19.00–100.00 ppm, excluding the dioxane signal at 69.00–70.00 ppm. The  $^1\text{H}$  NMR spectra were integrated in the range 1.30–9.50 ppm, excluding the interval 4.70–4.90 ppm containing the residual water signal and the interval 3.74–3.79 ppm containing the dioxane signal.

**Statistics.** All the data were analyzed by using the mixed procedure of SAS (SAS Institute Inc., Cary, NC) according to the model

$$Y_{ij} = \mu + \alpha_i + v_j + \varepsilon_{ij}$$

where  $Y_{ij}$  is the observed variable (i.e. the integral values of the NMR spectra: e.g., alanine),  $\mu$  is the overall mean,  $\alpha_i$  is the effect of treatment ( $i = 0, 100, 500 \mu\text{M H}_2\text{O}_2$ ),  $v_j$  is a random component incorporated to account for repeated measurements ( $j = 1, 2, 3$ ), and  $\varepsilon_{ij}$  is the residual error component. The random and residual error components were assumed to be independent and normally distributed, and their expectations were assumed to be zero. The absorbance measured after WST-1 addition (indication of cell viability) was also analyzed as described above in a model with the concentration of  $\text{H}_2\text{O}_2$  as a fixed effect and replicates as a random effect. Data are presented as least-squares means (LSMeans)  $\pm$  standard

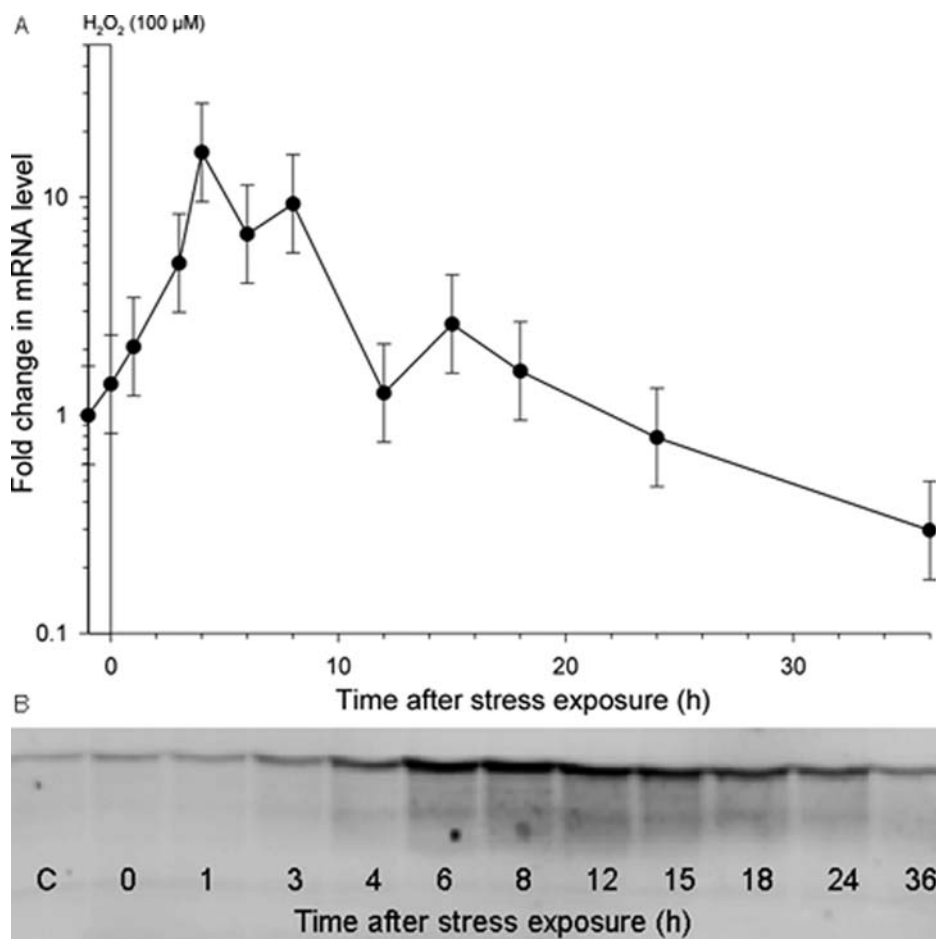


**Figure 2.** Fold changes in HO-1 mRNA level with 95%-CI (A) and changes in HO-1 protein expression (B) in C2C12 myotubes after 100  $\mu\text{M H}_2\text{O}_2$  oxidative stress exposure for 1 h. The control samples (C) are harvested after incubation in Krebs-HEPES buffer without  $\text{H}_2\text{O}_2$  for 1 h. The mRNA level is expressed relative to cells without stress (C).

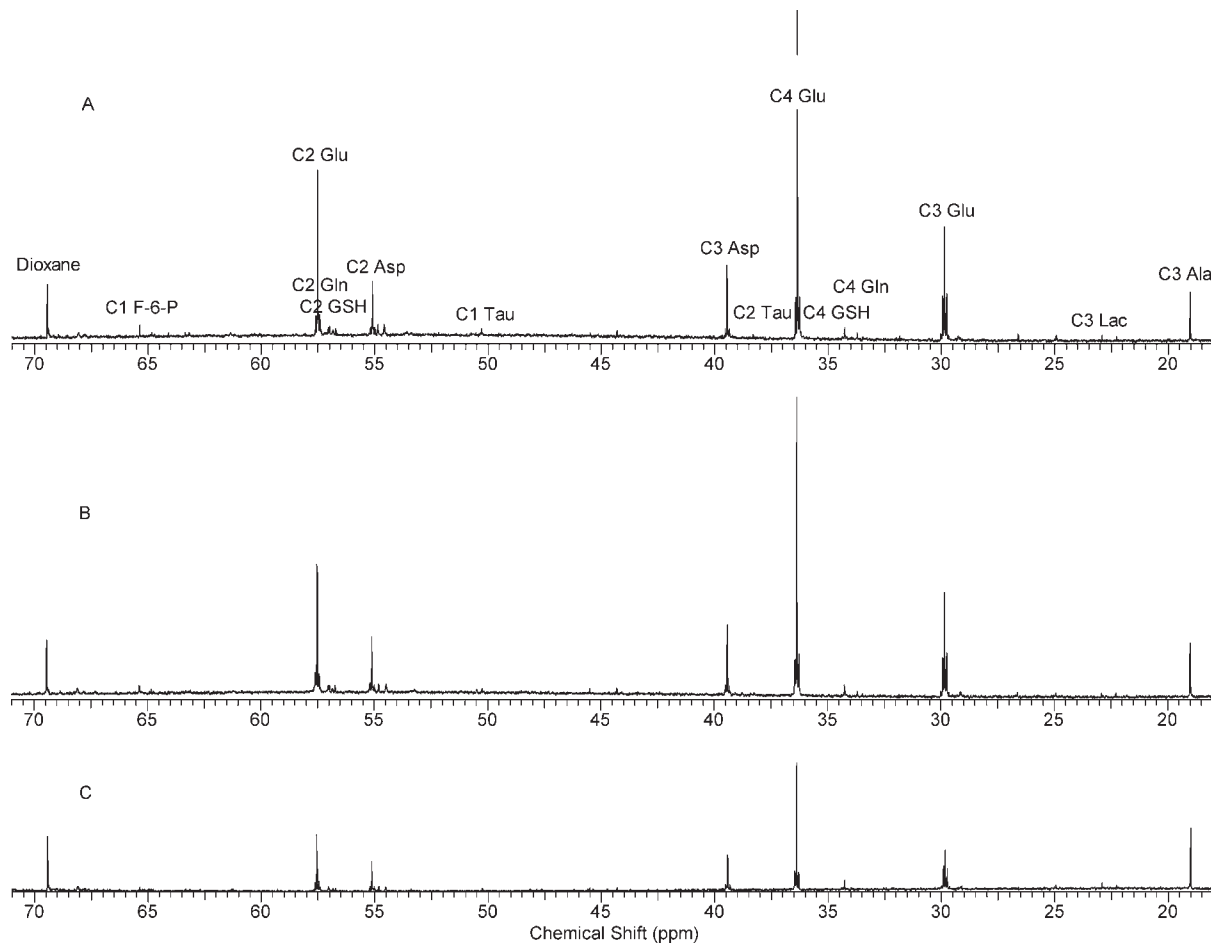


**Figure 3.**  $^{13}\text{C}$  NMR spectra of C2C12 mouse myotubes after incubation with  $^{13}\text{C}_1$ glucose for 4 h. The spectra were obtained on the freeze-dried methanol/water extractions of the cells: (A) control; (B)  $100\ \mu\text{M}$   $\text{H}_2\text{O}_2$  for 1 h; (C)  $500\ \mu\text{M}$   $\text{H}_2\text{O}_2$  for 1 h. Abbreviations: F-6-P, fructose-6-phosphate; Glu, glutamate; Gln, glutamine; GSH,  $\gamma$ -glutamyl-glutathione; Asp, aspartate; Tau, taurine; Lac, lactate; Ala, alanine. Dioxane is an internal reference.

errors of LSMeans (SEM). The level of HO-1 mRNA was analyzed in a model with time points as a fixed effect and replicates as a random effect. For quantification of mRNA, normalization was achieved by adjusting the RNA level for all samples to the same concentration ( $9\ \text{ng}/\mu\text{L}$ ), as described above. Data are presented as least-squares means (LSMeans)  $\pm$  95% confidence interval (CI).

## RESULTS

**Viability of Muscle Myotubes Exposed to  $\text{H}_2\text{O}_2$  Oxidative Stress.** The viability of the myotubes was examined after exposure to  $\text{H}_2\text{O}_2$  for 1 h, with concentrations varying between 0 and  $300\ \mu\text{M}$ . **Figure 1** shows that concentrations of up to  $100\ \mu\text{M}$   $\text{H}_2\text{O}_2$  caused no change in the viability of the myotubes. At concentrations above  $100\ \mu\text{M}$   $\text{H}_2\text{O}_2$  a decrease in the viability was observed.

**Effects of Oxidative Stress on HO-1 mRNA Level and HO-1 Protein Expression.** Changes in the level of HO-1 mRNA and expression of HO-1 protein over time, after the myotubes were exposed to  $100\ \mu\text{M}$   $\text{H}_2\text{O}_2$  for 1 h, were investigated with real-time RT-PCR and Western blot, respectively. From **Figure 2** it is apparent that the HO-1 mRNA level peaked 4 h after stress exposure, with an approximately 15-fold higher transcription in comparison to the control cells. The mRNA level was back to the baseline 24 h after stress exposure. The pattern of the HO-1 protein expression was comparable to that observed for HO-1 transcription. The expression of the protein peaked 6–8 h after stress exposure; thereafter it decreased toward the baseline within the 36 h time frame investigated.

**$^{13}\text{C}$ ,  $^1\text{H}$ , and  $^{31}\text{P}$  NMR Spectra.** After the myotubes were incubated with  $^{13}\text{C}_1$ glucose for 4 h under standard conditions,

the  $^{13}\text{C}$  label was found mainly in  $^{13}\text{C}_3$ alanine, in  $^{13}\text{C}_2$ ,  $^{13}\text{C}_3$ , and  $^{13}\text{C}_4$ glutamate, and in  $^{13}\text{C}_2$ - and  $^{13}\text{C}_3$ aspartate (**Figure 3** and **Table 1**). Labeling was also identified for  $^{13}\text{C}_3$ lactate,  $^{13}\text{C}_2$ - and  $^{13}\text{C}_4$ glutamine,  $^{13}\text{C}_2$ - and  $^{13}\text{C}_4$  $\gamma$ -glutamyl-glutathione,  $^{13}\text{C}_1$ fructose-6-phosphate, and  $^{13}\text{C}_1$  $\alpha$ - and  $^{13}\text{C}_1$  $\beta$ -glucose (not shown in **Figure 3**). Furthermore, small signals (average signal-to-noise ratio of  $\sim 5$  for the control samples) from naturally abundant  $^{13}\text{C}$  taurine were also detected. Under standard incubation conditions, several of the metabolites identified in the  $^{13}\text{C}$  NMR spectra and additional metabolites were identified in the  $^1\text{H}$  NMR spectra (**Figure 4** and **Table 2**) and in the  $^{31}\text{P}$  NMR spectra (**Figure 5**), respectively.

**Effects of Oxidative Stress on the Metabolite Levels.** Oxidative stress resulted in lower levels or tendencies to lower levels of several metabolites, including  $\gamma$ -glutamyl-glutathione (**Figure 3** and **Table 1**), glutamate, aspartate, glutamine, and taurine (**Figure 3**, **Tables 1** and **2**), fructose-6-phosphate (**Figure 3**, **Table 1**, and **Figure 5**), creatine, tyrosine, and phenylalanine (**Table 2**), and phosphocreatine (PCr), ATP, ADP, and  $\text{NAD}^+$  (**Table 2** and **Figure 5**). The decreases in the metabolites were generally small at  $100\ \mu\text{M}$   $\text{H}_2\text{O}_2$  stress exposure and were more pronounced after exposure to  $500\ \mu\text{M}$   $\text{H}_2\text{O}_2$ , and for the metabolites glutamate and glutamine the decreases were significant after exposure to  $500\ \mu\text{M}$   $\text{H}_2\text{O}_2$  (**Table 1**).

Conversely, higher levels of alanine were apparent in the  $^{13}\text{C}$  spectra (**Figure 3** and **Table 1**), and after exposure to  $500\ \mu\text{M}$   $\text{H}_2\text{O}_2$  the increase in alanine became significant (**Table 1**). In the  $^{13}\text{C}$  NMR spectra higher levels of  $^{13}\text{C}_3$ lactate were observed after

**Table 1.**  $^{13}\text{C}$  NMR Chemical Shift Ranges and LSmeans of the Absolute Integral Intensities, with Calculated Standard Error of the LSmeans (SEM)

metabolite	shift range (ppm)	LSmean			SEM
		control ( $n = 3$ )	100 $\mu\text{M}$ $\text{H}_2\text{O}_2$ ( $n = 3$ )	500 $\mu\text{M}$ $\text{H}_2\text{O}_2$ ( $n = 3$ )	
C <sub>3</sub> alanine	18.99–19.03	3.21	3.65	5.15 <sup>a</sup>	0.48
C <sub>3</sub> lactate	22.90–22.94	0.37	0.56	0.69	0.20
C <sub>3</sub> glutamate	29.81–29.87	14.27	13.89	8.74 <sup>a</sup>	1.34
C <sub>4</sub> glutamine	33.69–33.72	0.38	0.23	0.06 <sup>a</sup>	0.06
C <sub>4</sub> $\gamma$ -glutamyl-glutathione	34.24–34.28	1.50	1.22	1.00	0.19
C <sub>4</sub> glutamate	36.34–36.39	26.87	26.07	15.31 <sup>a</sup>	2.44
C <sub>2</sub> taurine	38.25–38.29	0.12	0.07	0.02	0.08
C <sub>3</sub> aspartate	39.40–39.45	5.20	5.80	4.23	0.92
C <sub>1</sub> taurine	50.21–50.29	0.56	0.34	0.01	0.38
C <sub>2</sub> aspartate	55.08–55.13	4.39	4.49	2.42	1.60
C <sub>2</sub> $\gamma$ -glutamyl-glutathione	56.83–56.85	0.82	0.63	0.01	0.56
C <sub>2</sub> glutamine	57.01–57.05	1.39	0.95	0.01	0.68
C <sub>2</sub> glutamate	57.51–57.55	13.14	12.37	5.74 <sup>a</sup>	1.90
C <sub>1</sub> fructose-6-phosphate	65.35–65.38	0.55	0.55	0.12	0.33
C <sub>1</sub> $\alpha$ -glucose	94.92–94.97	0.33	0.37	0.45	0.12
C <sub>1</sub> $\beta$ -glucose	98.75–98.78	0.28	0.56	0.58	0.19

<sup>a</sup>LSmeans differ significantly ( $P < 0.05$ ) on comparison with the control cells.

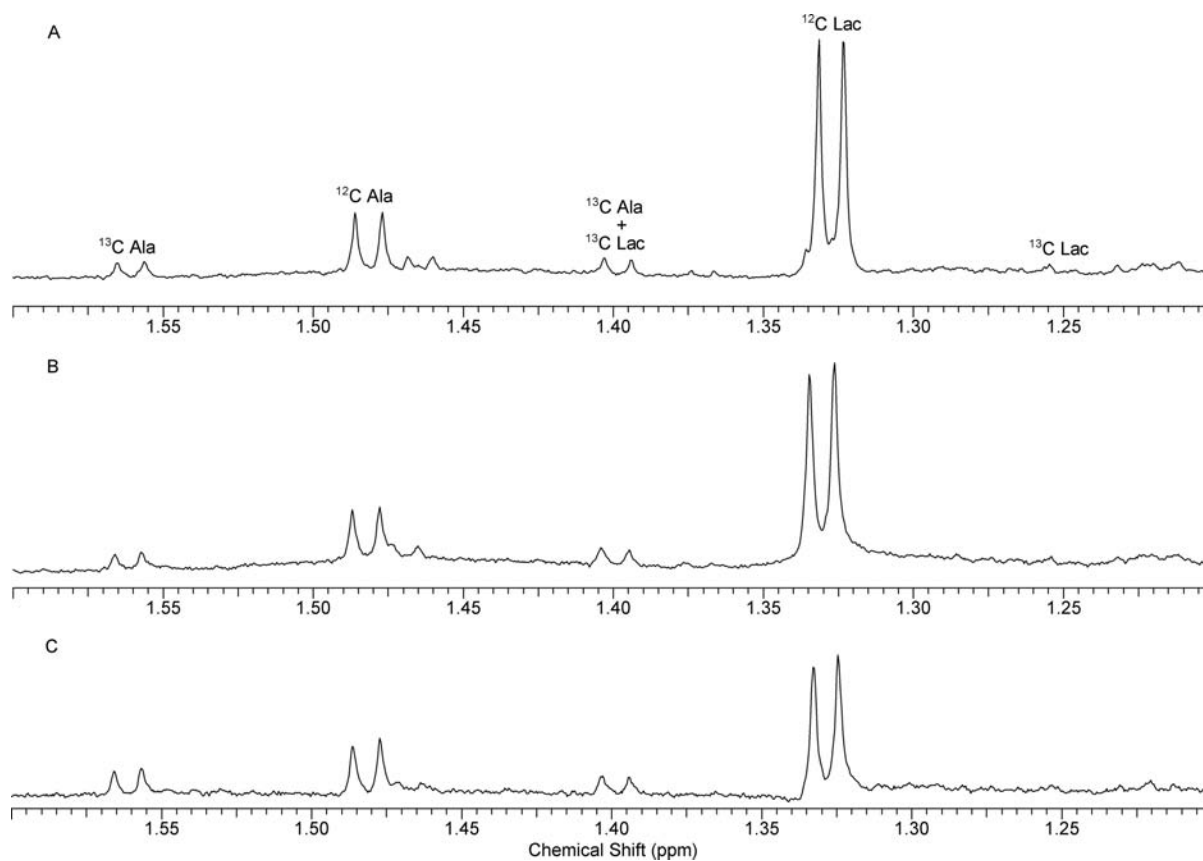


**Figure 4.** Expanded region showing lactate (Lac) and alanine (Ala) signals in the  $^1\text{H}$  NMR spectra of C2C12 mouse myotubes after incubation with [ $^{13}\text{C}_1$ ]glucose for 4 h: (A) control; (B) 100  $\mu\text{M}$   $\text{H}_2\text{O}_2$  for 1 h; (C) 500  $\mu\text{M}$   $\text{H}_2\text{O}_2$  for 1 h. The spectra were obtained on the freeze-dried methanol/water extractions of the cells. The satellite duplet for  $^{13}\text{C}$ -labeled lactate at  $\sim 1.40$  ppm is overlapping with the satellite duplet for  $^{13}\text{C}$ -labeled alanine, and hence the integral values for these duplets are not given. The integral values for the  $^{13}\text{C}$ -labeled alanine duplet at  $\sim 1.56$  ppm are given in **Table 2**. Due to low signal intensity, the integral values for the  $^{13}\text{C}$ -labeled lactate duplet at  $\sim 1.25$  ppm are not given in **Table 2**.

exposure to increasing concentrations of  $\text{H}_2\text{O}_2$  (**Figure 3** and **Table 1**). Conversely, lower levels of the unlabeled ( $^{12}\text{C}$ ) lactate were identified after stress exposure (**Figure 4** and **Table 2**).

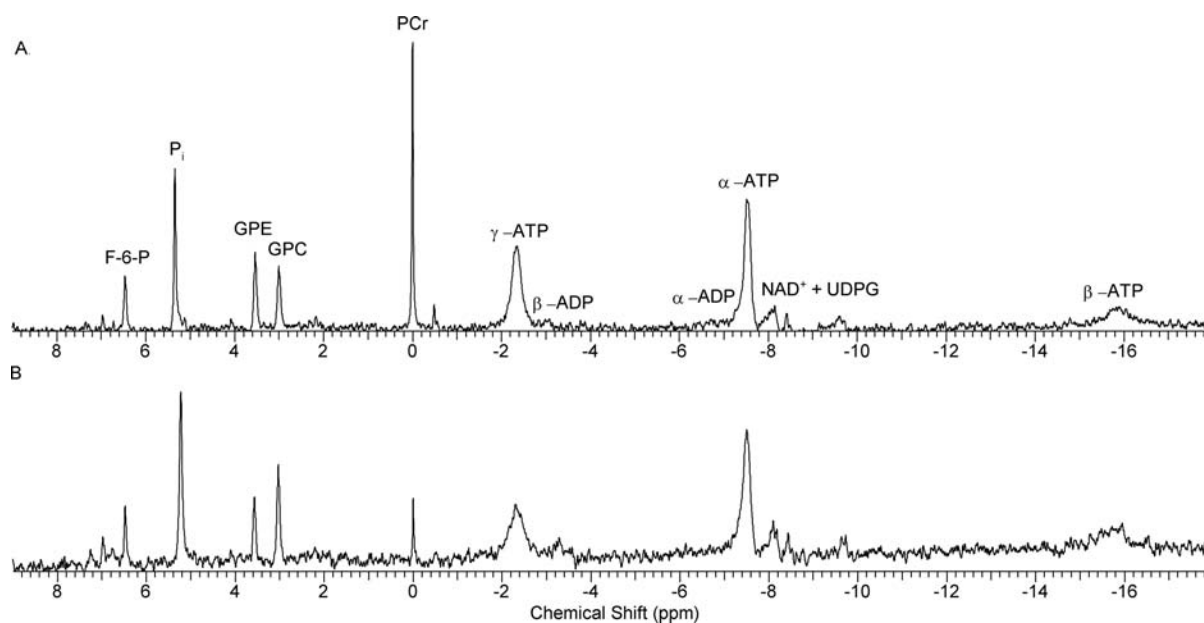
## DISCUSSION

The slaughter procedure comprises many types of stressors; both psychological and physical stressors are involved, and these

are exerted as both acute and long-term stressors. Taking a holistic approach is the obvious choice, as this resembles reality. However, the advantage of using model systems is the possibility to study one stressor at a time and then at a later stage collect all the information in order to compile a more complete picture of various stress-induced effects. When model systems are used, conditions are often applied that are more extreme than what is

**Table 2.**  $^1\text{H}$  NMR Chemical Shift Ranges and LSMeans of the Absolute Integral Intensities, with Calculated Standard Error of the LSMeans (SEM)

metabolite	shift range (ppm)	LSmean			SEM
		control ( $n = 3$ )	100 $\mu\text{M}$ $\text{H}_2\text{O}_2$ ( $n = 3$ )	500 $\mu\text{M}$ $\text{H}_2\text{O}_2$ ( $n = 3$ )	
lactate ( $\text{CH}_3$ ) (unlabeled)	1.32–1.33	0.73	0.65	0.55	0.14
alanine ( $\text{CH}_3$ ) (unlabeled)	1.48–1.49	0.21	0.21	0.20	0.06
alanine ( $\text{CH}_3$ ) ( $^{13}\text{C}$ labeled)	1.56–1.57	0.08	0.08	0.10	0.04
glutamate ( $\beta\text{-CH}_2$ )	2.05–2.06	1.34	1.23	0.86	0.29
glutamine ( $\beta\text{-CH}_2$ )	2.12–2.13	1.54	1.36	0.81	0.33
glutamate ( $\gamma\text{-CH}_2$ )	2.35–2.36	1.14	1.05	0.67	0.29
glutamine ( $\gamma\text{-CH}_2$ )	2.45–2.46	0.65	0.45	0.24	0.15
aspartate ( $\beta\text{-CH}_2$ )	2.81–2.82	0.63	0.50	0.48	0.17
taurine ( $\text{NCH}_2$ )	3.41–3.42	0.37	0.32	0.17	0.12
creatine ( $\text{CH}_2$ )	3.93–3.94	0.30	0.29	0.17	0.10
phosphocreatine ( $\text{CH}_2$ )	3.95–3.96	0.57	0.49	0.28	0.19
ATP/ADP (ribose H1)	6.15–6.16	0.28	0.26	0.16	0.07
tyrosine (H3/H5)	6.90–7.20	0.14	0.12	0.10	0.03
phenylalanine (H2/H6/H4/H/H5)	7.38–7.41	0.20	0.20	0.16	0.04
ATP/ADP (ring H2)	8.27–8.28	0.27	0.25	0.19	0.06
ATP/ADP (ring H8)	8.53–8.54	0.30	0.30	0.21	0.06
$\text{NAD}^+$	9.33–9.34	0.03	0.03	0.02	0.01

**Figure 5.**  $^{31}\text{P}$  NMR spectra of C2C12 mouse myotubes obtained on the freeze-dried methanol/water phase of the cell extractions: (A) control; (B) 500  $\mu\text{M}$   $\text{H}_2\text{O}_2$  for 1 h. Abbreviations: F-6-P, fructose-6-phosphate;  $\text{P}_i$ , inorganic phosphate; GPE, glycerophosphorylethanolamine; GPC, glycerophosphocholine; PCr, phosphocreatine.

apparent under physiological conditions. This is done in order to get more clear and distinguishable results, assisting in the identification of regulated compounds.

Expression of HO-1 protein has been applied as a marker for oxidative stress in skeletal muscles (26), and exposure to  $\text{H}_2\text{O}_2$  has also been shown to increase HO-1 mRNA level in cardiomyocytes (27). In the present study, we initially identified stress conditions under which the myotubes maintained full viability. This was the case at 100  $\mu\text{M}$   $\text{H}_2\text{O}_2$  for 1 h (Figure 1), and under these stress conditions an increase in the mRNA level of HO-1 was seen (Figure 2). The expression of HO-1 protein also increased after exposure to  $\text{H}_2\text{O}_2$  oxidative stress, peaking with a time delay of 2–4 h in comparison to the peak in the mRNA level. From these results it is apparent that an oxidative stress level of 100  $\mu\text{M}$   $\text{H}_2\text{O}_2$  causes an upregulation of the HO-1 mRNA level, resulting in increased expression of HO-1 protein. At a 100  $\mu\text{M}$   $\text{H}_2\text{O}_2$  stress exposure the viability of the myotubes was

not decreased, and the cellular disturbance at this stress level is apparently reversible, since the HO-1 mRNA level returned to baseline within 24 h and the HO-1 protein level almost reversed to baseline within the 36 h time frame investigated.

From the initial results of the NMR spectroscopic data it was apparent that 100  $\mu\text{M}$   $\text{H}_2\text{O}_2$  caused only minor changes in the metabolite levels. Hence, a more extreme oxidative stress exposure of 500  $\mu\text{M}$   $\text{H}_2\text{O}_2$  was also applied in the NMR experiments, in addition to the concentration of 100  $\mu\text{M}$ . In accordance with previous experiments of heat and anoxia stressed C2C12 myotubes (22), the metabolites identified in the  $^{13}\text{C}$ ,  $^1\text{H}$ , and  $^{31}\text{P}$  NMR spectra in the present study were primarily metabolites derived from the glycolysis and the Krebs cycle (Figure 6).  $^{13}\text{C}$  was mainly incorporated in the cytosolic-derived metabolite alanine and the mitochondrial-derived metabolites glutamate and aspartate. Oxidative stress resulted in lower levels of glutamate and aspartate, indicating impairment of the mitochondrial function.

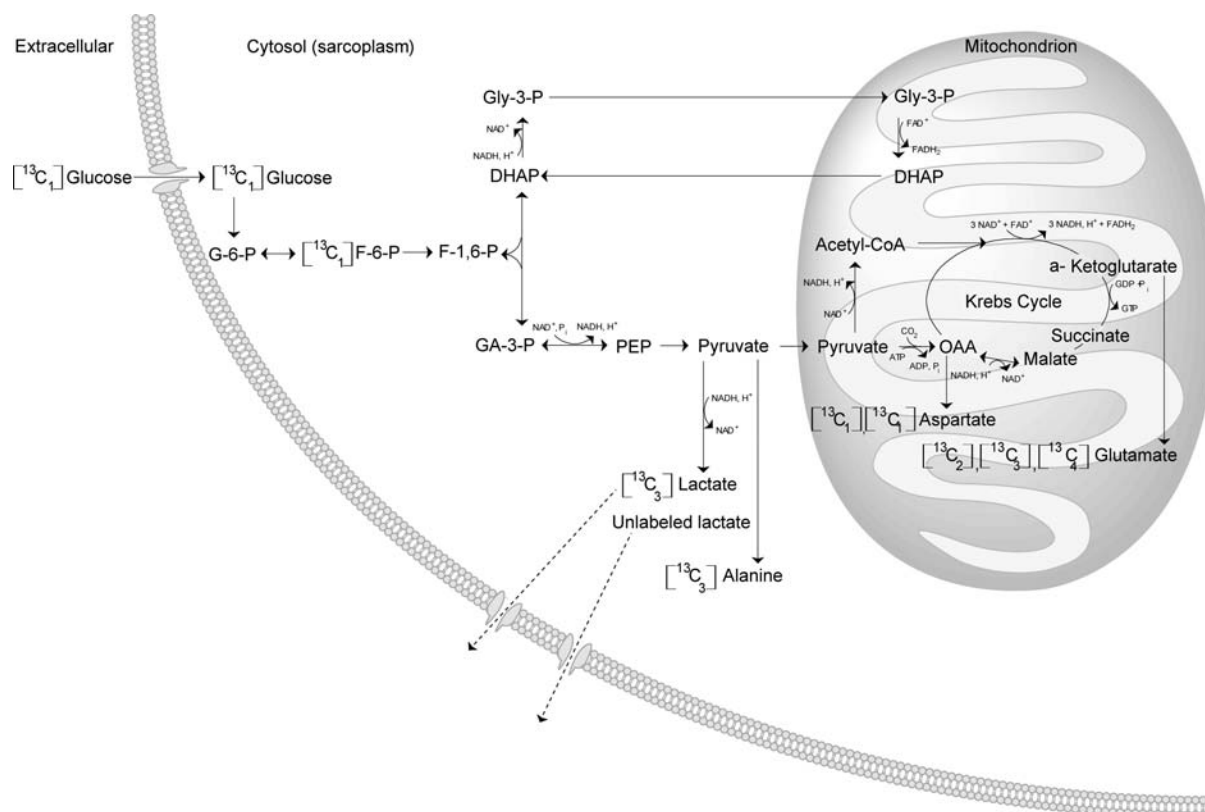


**Figure 6.** Schematic representation of the main reactions involved in  $^{13}\text{C}_1$  glucose metabolism in C2C12 mouse myotubes. At standard incubation conditions pyruvate is oxidized in the Krebs cycle. When exposed to oxidative stress  $^{13}\text{C}_1$  lactate is produced through the anaerobic glycolytic pathway, and lactate is released from the myotubes to the medium. Solid arrows indicates metabolism of  $^{13}\text{C}_1$  glucose, whereas dashed arrows indicate release of metabolites. Abbreviations: Gly-3-P, glycerol-3-phosphate; DHAP, dihydroxyacetone phosphate; G-6-P, glucose-6-phosphate; F-6-P, fructose-6-phosphate; F-1,6-P, fructose-1,6-bisphosphate; GA-3-P, glyceraldehyde-3-phosphate; PEP, phosphoenolpyruvate; OAA, oxaloacetate.

In general, with increasing severity of stress, lower levels of almost all detected metabolites, which are mainly representing amino acids, were observed in the  $^{13}\text{C}$  and the  $^1\text{H}$  spectra. This is in agreement with previous experiments of heat and anoxia stressed C2C12 myotubes (22). These results indicate that both unlabeled ( $^{12}\text{C}$ ) amino acids and  $^{13}\text{C}$ -labeled amino acids are released from the myotubes to the medium, with increasing release at increasing severity of oxidative stress. Release of amino acids from human skeletal muscles into the bloodstream has also been observed after stress exposure induced by infusion of hormones (28) and when exposing patients with chronic heart failure to light physical exercise (29), respectively.

In agreement with the effect of stressful conditions observed in previous experiments (22), very small increases in lactate were observed in the  $^{13}\text{C}$  spectra at increasing concentrations of  $\text{H}_2\text{O}_2$  exposure (Figure 3 and Table 1). In the  $^1\text{H}$  NMR spectra, in contrast to the  $^{13}\text{C}$  NMR spectra, even lower levels of lactate designated by the peaks at a chemical shift of 1.32–1.33 ppm, representing unlabeled ( $^{12}\text{C}$ ) lactate, were observed with increasing concentrations of  $\text{H}_2\text{O}_2$  exposure (Figure 4 and Table 2). These results should probably be explained by release of lactate from the myotubes, as illustrated in Figure 6. Thus, the results are also in agreement with findings in C2C12 myoblasts and myotubes under anoxic conditions (9, 30) and in skeletal muscles stimulated with hormones (28), which in both cases resulted in release of lactate. In recent experiments applying  $^1\text{H}$  NMR metabolomics on plasma from pigs that were exercised on a treadmill and fish that were exposed to handling stress, respectively, the metabolite primarily released to the blood was lactate (31, 32), providing further support to the hypothesis in the

present experiment that lactate is released to the medium under oxidative stress conditions.

Only one amino acid (alanine) increased upon oxidative stress, as observed for the  $^{13}\text{C}$ -labeled alanine in both the  $^{13}\text{C}$  spectra and the  $^1\text{H}$  spectra (Figure 3, Table 1, Figure 4 and Table 2). In the  $^1\text{H}$  spectra no changes in the unlabeled ( $^{12}\text{C}$ ) alanine were apparent (Figure 4 and Table 2), which indicate that oxidative stress causes an increase in de novo synthesis of alanine. In rabbit hearts an increase in de novo synthesis of alanine has been observed under anoxic conditions, concomitant with a decrease in glutamate (33). Taegtmeier et al. (33) hypothesized that under anoxic stress conditions pyruvate could be shunted to alanine production instead of lactate production, which is in agreement with the increase in the de novo synthesis of alanine, concomitant with a very small accumulation of de novo synthesized lactate in the present study. The decrease in glutamate and other amino acids, concomitant with an increase in alanine, also indicates the conversion of these amino acids through different entries into the Krebs cycle, which results in additional energy production. This could also partly explain the general decrease in all amino acids except for alanine itself.

In a study by Zeng et al. (34) cerebrocortical slices from rats were exposed to 2 mM  $\text{H}_2\text{O}_2$  oxidative stress for 1 h. On examination with  $^1\text{H}$  NMR spectroscopy after a 4 h recovery period, Zeng et al. (34) observed that oxidative stress tended to show decreases in all metabolites, in comparison to control samples, except for lactate and alanine, which did not change.

Oxidative stress caused lower levels of ATP/ADP and PCr, as identified in the  $^1\text{H}$  NMR spectra, and the reduction in PCr was confirmed in the  $^{31}\text{P}$  NMR spectra. These changes in ATP, ADP,

and PCr are in agreement with our previous observations in mouse myotubes under heat and anoxic conditions (22). However, the oxidative stress in the present experiments only caused a severe decrease in the high-energy phosphate PCr, whereas the decreases in ATP and ADP were barely detectable (Table 2 and Figure 5). These findings are in agreement with  $^{31}\text{P}$  NMR observations by Brand et al. (19) in rat brain astrocytes exposed to 200  $\mu\text{M}$   $\text{H}_2\text{O}_2$  oxidative stress. They observed a severe breakdown of energy metabolism immediately after  $\text{H}_2\text{O}_2$  treatment, resulting in lower levels of ATP and PCr concentrations below NMR detectability, while already after a 2 h recovery period the ATP level had restored, and the PCr level had partly restored.

In addition to changes in metabolites related to the glycolysis and the Krebs cycle, also changes in taurine levels were observed both in the  $^1\text{H}$  NMR spectra and in the natural  $^{13}\text{C}$ -containing taurine in the  $^{13}\text{C}$  NMR spectra under stress conditions. Lower levels of taurine were apparent in the myotubes at increasing concentrations of  $\text{H}_2\text{O}_2$  exposure. Reduction of taurine under anoxic conditions in muscle myotubes is thought to be caused by release of taurine from the cells, induced by reactive oxygen species (ROS) (12). Also in rat brain astrocytes reduced levels of taurine in  $^1\text{H}$  NMR spectra were observed after exposure to 200  $\mu\text{M}$   $\text{H}_2\text{O}_2$ ; hence, oxidative stress causes a dysregulation of the osmotic control, resulting in release of taurine (19).

The regulation at the metabolite level monitored with  $^{13}\text{C}$ ,  $^1\text{H}$ , and  $^{31}\text{P}$  NMR spectroscopy was not as apparent as the regulation of the mRNA level and the protein expression, when determined with real time RT-PCR and Western blot, respectively, even when an oxidative stress level of 500  $\mu\text{M}$   $\text{H}_2\text{O}_2$  was applied. The changes in the metabolite levels when the myotubes were exposed to 500  $\mu\text{M}$  were also seen very weakly at an oxidative stress level of 100  $\mu\text{M}$ ; however, the decreases or increases in metabolite level were never significantly different from the control myotubes. From the experiments by Brand et al. (19) on brain astrocytes it is apparent that the time point after  $\text{H}_2\text{O}_2$  oxidative stress exposure is very critical for identifying effects of the stress exposure, since the changes in metabolite level vary markedly at different time points after stress exposure. Brand et al. (19) found that the changes in metabolites in general were largest immediately after oxidative stress exposure; however, the recovery time for the different metabolites varied, being fastest for the high-energy metabolites, which recovered within a few hours, whereas the osmolytes and the metabolites derived from complex glucose metabolism recovered much more slowly within a 24 h period. The NMR spectroscopic data in the present experiment were acquired at only one time point (3 h after stress exposure); hence, it cannot be ruled out that analyzing with NMR spectroscopy at other time points, e.g. at earlier time points, could result in more apparent differences between control myotubes and myotubes exposed to oxidative stress. The present results indicate that changes in mRNA level or protein expression can be detected at lower levels of oxidative stress exposure compared to detection in changes of metabolite levels. However, the NMR spectroscopic methods have the advantage that multiple metabolites are monitored simultaneously, and some of these have a close link to meat quality: e.g., lactate (6, 7, 32). Hence, upregulation of HO-1 mRNA or protein or changes in metabolite levels could possibly be useful as markers for meat quality traits.

From the present study it is apparent that oxidative stress influences the cellular activity at many levels in muscle myotubes. It was found that oxidative stress influences the transcription and thereby the expression of HO-1. With the metabolomic approach combining NMR spectroscopy on three different nuclei, it was apparent that oxidative stress influences the levels of metabolites derived from complex glucose metabolism, high-energy metabolites,

and also the release rates of metabolites. These results indicate that the cellular mechanisms are influenced at many levels under stressful conditions apparent in relation to slaughter. Hence, the knowledge about the basic regulation mechanisms gained in the present study by applying oxidative stress in a muscle model system could be useful in future studies of stress in relation to slaughter in studies applying a more holistic approach.

#### ABBREVIATIONS USED

CI, confidence interval; COSY, correlation spectroscopy; DMEM, Dulbecco's Modified Eagle's Medium; FCS, fetal calf serum; FID, free induction decays; HO-1, heme oxygenase-1; HSQC, heteronuclear single-quantum coherence spectroscopy; LSM, least-squares means; MAS, magic angle spinning; PBS, phosphate-buffered saline; PCr, phosphocreatine; ROS, reactive oxygen species; RT-PCR, reverse transcription polymerase chain reaction; SEM, standard errors of LSM; TTBS, Tween-Tris-buffered saline.

#### ACKNOWLEDGMENT

Sebastian Meyer is acknowledged for technical assistance, and Anne-Grete Dyrvig Petersen and Inge Lise Sørensen are thanked for their laboratory assistance and for valuable discussions. The 800 MHz spectra were obtained using the Bruker 800 spectrometer of the Danish Instrument Center for NMR Spectroscopy of Biological Macromolecules.

#### LITERATURE CITED

- (1) van der Wal, P. G.; Engel, B.; Reimert, H. G. M. The effect of stress, applied immediately before stunning, on pork quality. *Meat Sci.* **1999**, *53*, 101–106.
- (2) Kuchenmeister, U.; Kuhn, G.; Ender, K. Preslaughter handling of pigs and the effect on heart rate, meat quality, including tenderness, and sarcoplasmic reticulum  $\text{Ca}^{2+}$  transport. *Meat Sci.* **2005**, *71*, 690–695.
- (3) Young, J. F.; Bertram, H. C.; Oksbjerg, N. Rest before slaughter ameliorates pre-slaughter stress-induced increased drip loss but not stress-induced increase in the toughness of pork. *Meat Sci.* **2009**, *83*, 634–641.
- (4) Grandin, T. The effect of stress on livestock and meat quality prior to and during slaughter. *Int. J. Stud. Anim. Prob.* **1980**, *1*, 313–337.
- (5) Terlouw, C. Stress reactions at slaughter and meat quality in pigs: genetic background and prior experience - A brief review of recent. *Livest. Prod. Sci.* **2005**, *94*, 125–135.
- (6) Schafer, A.; Rosenvold, K.; Purslow, P. P.; Andersen, H. J.; Henckel, P. Physiological and structural events postmortem of importance for drip loss in pork. *Meat Sci.* **2002**, *61*, 355–366.
- (7) Stoier, S.; Aaslyng, M. D.; Olsen, E. V.; Henckel, P. The effect of stress during lairage and stunning on muscle metabolism and drip loss in Danish pork. *Meat Sci.* **2001**, *59*, 127–131.
- (8) Young, J. F.; Hansen-Møller, J.; Oksbjerg, N. Effect of flavonoids on stress responses in myotube cultures. *J. Agric. Food Chem.* **2004**, *52*, 7158–7163.
- (9) Gawlitta, D.; Oomens, C. W. J.; Bader, D. L.; Baaijens, F. P. T.; Bouten, C. V. C. Temporal differences in the influence of ischemic factors and deformation on the metabolism of engineered skeletal muscle. *J. Appl. Physiol.* **2007**, *103*, 464–473.
- (10) Siu, P. M.; Wang, Y.; Alway, S. E. Apoptotic signaling induced by  $\text{H}_2\text{O}_2$ -mediated oxidative stress in differentiated C2C12 myotubes. *Life Sci.* **2009**, *84*, 468–481.
- (11) Lambert, I. H.; Nielsen, J. H.; Andersen, H. J.; Ortenblad, N. Cellular model for induction of drip loss in meat. *J. Agric. Food Chem.* **2001**, *49*, 4876–4883.
- (12) Ortenblad, N.; Young, J. F.; Oksbjerg, N.; Nielsen, J. H.; Lambert, I. H. Reactive oxygen species are important mediators of taurine release from skeletal muscle cells. *Am. J. Physiol.: Cell Physiol.* **2003**, *284*, C1362–C1373.



- (13) VanDenThillart, G.; VanWaarde, A. Nuclear magnetic resonance spectroscopy of living systems: Applications in comparative physiology. *Physiol. Rev.* **1996**, *76*, 799–837.
- (14) Halliwell, B. The wanderings of a free radical. *Free Radic. Biol. Med.* **2009**, *46*, 531–542.
- (15) Bertram, H. C.; Stodkilde-Jorgensen, H.; Karlsson, A. H.; Andersen, H. J. Post mortem energy metabolism and meat quality of porcine M-longissimus dorsi as influenced by stunning method - A P-31 NMR spectroscopic study. *Meat Sci.* **2002**, *62*, 113–119.
- (16) Bertram, H. C.; Jakobsen, H. J.; Andersen, H. J.; Karlsson, A. H.; Engelsen, S. B. Post-mortem changes in porcine M. longissimus studied by solid-state C-13 cross-polarization magic-angle spinning nuclear magnetic resonance spectroscopy. *J. Agric. Food Chem.* **2003**, *51*, 2064–2069.
- (17) Bertram, H. C.; Jakobsen, H. J.; Andersen, H. J. Combined high-field C-13 CP MAS NMR and low-field NMR relaxation measurements on post mortem porcine muscles. *J. Agric. Food Chem.* **2004**, *52*, 3159–3164.
- (18) Bertram, H. C.; Whittaker, A. K.; Andersen, H. J.; Karlsson, A. H. The use of simultaneous H-1 & P-31 magic angle spinning nuclear magnetic resonance measurements to characterize energy metabolism during the conversion of muscle to meat. *Int. J. Food Sci. Technol.* **2004**, *39*, 661–670.
- (19) Brand, A.; Leibfritz, D.; Richter-Landsberg, C. Oxidative stress-induced metabolic alterations in rat brain astrocytes studied by multinuclear NMR spectroscopy. *J. Neurosci. Res.* **1999**, *58*, 576–585.
- (20) Perrin, A.; Roudier, E.; Duborjal, H.; Bachelet, C.; Riva-Lavieille, C.; Leverve, X.; Massarelli, R. Pyruvate reverses metabolic effects produced by hypoxia in glioma and hepatoma cell cultures. *Biochimie* **2002**, *84*, 1003–1011.
- (21) Brand, A.; Richterlandsberg, C.; Leibfritz, D. Multinuclear NMR-studies on the energy-metabolism of glial and neuronal cells. *Dev. Neurosci.* **1993**, *15*, 289–298.
- (22) Straadt, I. K.; Young, J. F.; Petersen, B. O.; Duus, J. O.; Gregersen, N.; Bross, P.; Oksbjerg, N.; Bertram, H. C. Metabolic profiling of heat or anoxic stress in mouse C2C12 myotubes using multinuclear NMR spectroscopy. *Metabolism* **2009**, DOI: 10.1016/j.metabol.2009.09.029.
- (23) Yaffe, D.; Saxel, O. Serial passaging and differentiation of myogenic cells isolated from dystrophic mouse muscle. *Nature* **1977**, *270*, 725–727.
- (24) Bustin, S. A. Quantification of mRNA using real-time reverse transcription PCR (RT-PCR): trends and problems. *J. Mol. Endocrinol.* **2002**, *29*.
- (25) Towbin, H.; Staehelin, T.; Gordon, J. Electrophoretic transfer of proteins from polyacrylamide gels to nitrocellulose sheets - procedure and some applications. *Proc. Natl. Acad. Sci. U.S.A.* **1979**, *76*, 4350–4354.
- (26) Tarricone, E.; Scapin, C.; Vitadello, M.; Esposito, F.; Margonato, V.; Milano, G.; Samaja, M.; Gorza, L. Cellular distribution of Hsp70 expression in rat skeletal muscles. Effects of moderate exercise training and chronic hypoxia. *Cell Stress Chaperones* **2008**, *13*, 483–495.
- (27) Borger, D. R.; Essig, D. A. Induction of HSP 32 gene in hypoxic cardiomyocytes is attenuated by treatment with N-acetyl-L-cysteine. *Am. J. Physiol.: Heart Circ. Physiol.* **1998**, *274*, H965–H973.
- (28) Brown, J.; Gore, D. C.; Lee, R. Dichloroacetate inhibits peripheral efflux of pyruvate and alanine during hormonally simulated catabolic stress. *J. Surg. Res.* **1993**, *54*, 592–596.
- (29) Aquilani, R.; Opasich, C.; Dossena, M.; Iadarola, P.; Gualco, A.; Arcidiaco, P.; Viglio, S.; Boschi, F.; Verri, M.; Pasini, E. Increased skeletal muscle amino acid release with light exercise in deconditioned patients with heart failure. *J. Am. Coll. Cardiol.* **2005**, *45*, 158–160.
- (30) Hwang, D. Y.; Ismail-Beigi, F. Glucose uptake and lactate production in cells exposed to CoCl<sub>2</sub> and in cells overexpressing the Glut-1 glucose transporter. *Arch. Biochem. Biophys.* **2002**, *399*, 206–211.
- (31) Karakach, T. K.; Huenupi, E. C.; Soo, E. C.; Walter, J. A.; Afonso, L. O. B. H-1-NMR and mass spectrometric characterization of the metabolic response of juvenile Atlantic salmon (*Salmo salar*) to long-term handling stress. *Metabolomics* **2009**, *5*, 123–137.
- (32) Bertram, H. C.; Oksbjerg, N.; Young, J. F. NMR-based metabolomics reveals relationship between pre-slaughter exercise stress, the plasma metabolite profile at time of slaughter, and water-holding capacity in pigs. *Meat Sci.* **2010**, *84*, 108–113.
- (33) Taetmeyer, H.; Peterson, M. B.; Ragavan, V. V.; Ferguson, A. G.; Lesch, M. Denovo alanine synthesis in isolated oxygen-deprived rabbit myocardium. *J. Biol. Chem.* **1977**, *252*, 5010–5018.
- (34) Zeng, J. Y.; Liu, J.; Yang, G. Y.; Kelly, M. J. S.; James, T. L.; Litt, L. Exogenous ethyl pyruvate versus pyruvate during metabolic recovery after oxidative stress in neonatal rat cerebroconical slices. *Anesthesiology* **2007**, *107*, 630–640.

---

Received for review October 6, 2009. Revised manuscript received December 22, 2009. Accepted December 26, 2009. The Danish Research Council FTP is gratefully acknowledged for financial support through the projects "Cellular stress and metabolic responses to ante- and post mortem stress factors elucidated in primary porcine muscle cell cultures using confocal microscopy and NMR-based metabolic profiling" (Project No. 274-06-0107) and "NMR-based metabolomics on tissues and biofluids" (Project No. 274-05-339).